BJR https://doi.org/10.1259/bjr.20180598

Received: 05 July 2018 | Revised: 03 November 2018 | Accepted: 09 November 2018

© 2019 The Authors. Published by the British Institute of Radiology under the terms of the Creative Commons Attribution-NonCommercial 4.0 Unported License http://creativecommons.org/licenses/by-nc/4.0/, which permits unrestricted non-commercial reuse, provided the original author and source are credited.

Cite this article as:
Xie Y, Zhang S, Liu J, Liang X, Zhang X, Zhang Y, et al. Value of CT spectral imaging in the differential diagnosis of thymoma and mediastinal lymphoma. *Br J Radiol* 2019; **92**: 20180598.

FULL PAPER

Value of CT spectral imaging in the differential diagnosis of thymoma and mediastinal lymphoma

[1]YIJING XIE, MMed, [2]SHIPENG ZHANG, MMed, [1]JIANLI LIU, MMed, [1]XIAOHONG LIANG, MMed, [1]XUELING ZHANG, MMed, [1]YUTING ZHANG, MMed, [3]ZHUOLI ZHANG, MMed and [1]JUNLIN ZHOU, MMed

[1]Department of Radiology, Lanzhou University Second Hospital, Lanzhou, PR China
[2]Department of Radiology, Gansu Provincial Maternity and Child-care hospital, Lanzhou, PR China
[3]Department of Radiology, Northwestern University, Chicago, USA

Address correspondence to: Mrs Yijing Xie
E-mail: *570742057@qq.com*

The authors Yijing Xie and Shipeng Zhang contributed equally to the work.

Objective: To investigate the imaging characteristics of thymoma and mediastinal lymphoma using spectral CT and evaluate whether the quantitative information can improve the differential diagnosis of these diseases.

Methods: This retrospective study was approved by the institutional review board, and written informed consent was obtained from all patients. Overall, 39 patients with mediastinal tumors (24 thymomas and 15 mediastinal lymphomas) were examined with CT spectral imaging during the arterial phase (AP) and venous phase (VP). Iodine concentrations were derived from iodine-based material-decomposition CT images and normalized to the iodine concentration in the aorta. The difference in normalized iodine concentrations (NICs), HU curve slop(λ_{HU}), and the differences between AP and VP for CT values of lesions in 70 Kev were calculated. The two-sample *t*-test was performed to compare quantitative parameters, and non-quantitative parameters were compared with the Chi-square test (Fisher exact). Receiver operating characteristic (ROC) curves were generated to help establish threshold values for the parameters required for the significant differentiation of thymomas from mediastinal lymphomas. Two readers qualitatively assessed the lesion types according to the imaging features. The sensitivity and specificity of the qualitative and quantitative studies were compared.

Results: NICs during the VP and λ_{HU} during the AP in patients with mediastinal lymphomas differed significantly from those in patients with thymomas. The mean NICs during the VP were 0.28 ± 0.08 mg ml^{-1} (±standard deviation) *vs* 0.49 ± 0.15 mg ml^{-1}, respectively. The λ_{HU} during the AP was 0.69 ± 0.17 *vs* 1.26 ± 0.74, respectively. The NICs during the VP and λ_{HU} during the AP had high sensitivity and specificity in differentiating mediastinal lymphomas from thymomas. The tumor location, margin, necrosis, presence of swollen mediastinal lymph nodes, relationship with adjacent vessels, and enhancement pattern differed significantly between the groups ($p < 0.05$). The combination of NICs and λ_{HU} had higher sensitivity and specificity than did those of conventional qualitative CT image analysis during the combined phases.

Conclusion: CT spectral imaging has promising potential for the diagnostic differentiation of mediastinal lymphomas and thymomas. The iodine content and λ_{HU} could be valuable parameters for differentiating thymomas and mediastinal lymphomas.

Advances in knowledge: The iodine content and λ_{HU}, provided by spectral CT, could be used as new parameters to distinguish mediastinal lymphomas from thymomas.

INTRODUCTION

Thymoma is a rare mediastinal neoplasm but is the most common primary neoplasm of the anterior mediastinum.[1] CT is the imaging modality of choice for evaluating thymoma and can help distinguish thymomas from other anterior mediastinal abnormalities. Because the completeness of resection is a major prognostic factor, surgical resection is the cornerstone of treatment of patients with thymoma.[2]

Mediastinal lymphoma is a lymphoma that is located in the anterior mediastinum and originated in the thymus or

lymph nodes.[3] Differentiating between thymoma and mediastinal lymphoma is essential because they require different therapeutic approaches. Surgical resection has been shown to be a highly effective treatment technique in patients with thymoma;[4] conversely, chemotherapy is justified in patients with mediastinal lymphoma.[5] However, there is considerable overlap between the imaging features of anterior mediastinal lymphoma and thymoma, and it is difficult to differentiate the diagnoses.

In recent years, quantitative mass spectrometry CT imaging has become a field of intense study. Spectral CT imaging with material decomposition reconstruction has enabled the transformation of conventional attenuation data into effective material densities, such as those of iodine and water.[6] This procedure theoretically allows two types of tumor to be differentiated on the basis of tumor iodine density after administering an iodine contrast agent because the amount of neovascularity is unequal.[7] This imaging method has been used in several clinical applications, including differentiating hepatocellular carcinoma and focal nodular hyperplasia of the liver[8] and identifying portal vein thrombosis and tumor thrombus.[9]

The purpose of this study was to investigate the value of CT spectral imaging in differentiating mediastinal lymphoma from thymoma.

METHODS AND MATERIALS

Patients and setting

The ethics committee at our institution approved this retrospective study, and all patients provided written informed consent. From June 2014 to June 2017, 87 patients who were known or suspected to have mediastinal tumors underwent non-enhanced CT and dual-phase contrast-enhanced CT in dual-energy spectral mode. A total of 48 patients were excluded from the study because they did not have mediastinal lymphoma or thymoma. A final cohort of 39 patients with anterior mediastinal tumor was included in the present study. 24 patients [19 males, 5 females; median age 55 ± 8 (42–69 years)] had thymoma, and 15 patients [11 males, 4 females; median age 39 ± 6 (29–50 years)] had mediastinal lymphoma. The thymomas in all 24 patients were proven pathologically after surgical resection. 9 of the 15 mediastinal lymphomas were proven by effective chemotherapy, and the other 6 lymphomas were confirmed histologically after needle biopsy due to diagnostic uncertainty, in which 4 of them were diffuse large B cell lymphoma, and 2 were *T*-lymphoblastic lymphoma.

CT examination

Triple-phase CT (*i.e.* unenhanced and two-phase contrast-enhanced CT examinations) was performed using a Discovery CT750 HD CT system (GE Healthcare, Waukesha, WI). All patients underwent imaging craniocaudally in the supine position. Unenhanced images were acquired following scout imaging with the conventional helical mode at a tube voltage of 120 kVp, tube current smart mA (100–500 mA, noise index 14.00), helical pitch:1.375, rotation time 0.7 s. Patients were then injected with a total of 80–100 ml non-ionic contrast medium (ioversol, 320 mg iodine ml^{-1}) via antecubital venous access at a rate of 3.5–4.0 ml s^{-1} during both the arterial phase (AP) and the venous phase (VP). AP scanning began 18 s after the trigger attenuation threshold [80 HU (Hounsfield units)] was reached at the level of the thoracic aorta. At a delay of 25 s after AP imaging, VP scanning began. AP and VP scanning were performed in the spectral imaging mode with fast tube voltage switching between 80 and 140 kVp on adjacent views during a single rotation. The other imaging parameters were as follows: collimation thickness 1.25 mm, tube current 275 mA, rotation speed 0.7 s, helical pitch 1.375, reconstructional standard 30% adaptive statistical iterative reconstruction. The CT images were reconstructed using projection-based material-decomposition software and a standard reconstruction kernel. The adaptive statistical iterative reconstruction algorithm was applied to suppress image noise on the decomposition images. Three types of images were reconstructed from the single spectral CT acquisition for analysis: conventional polychromatic images obtained at 140 kVp, water- and iodine-based material-decomposition images, and monochromatic images obtained at energies ranging from 40 to 140 keV.

Quantitative analysis

All the measurements were performed on an advanced workstation (AW4.6, Discovery CT 750 HD, GE Healthcare) with the Gemstone Spectral Imaging viewer. The default 70-keV monochromatic images and iodine-based material decomposition images were reviewed. Circular or elliptical regions of interests (ROI) with an area of approximately 100 mm^2 were marked on the lesions and aorta, with a default of 70 keV for monochromatic images. The ROIs encompassed as much of the high-enhancing areas of the lesions as possible. Areas of focal change, such as cystic degeneration, necrosis, calcification, and large vessels, were carefully avoided. To ensure consistency, all measurements were performed three times at different image levels, and the average values were calculated. For all measurements, the size, shape and position of the ROIs were kept consistent between the phases by applying the copy-paste function. The GSI viewer software package automatically calculated the CT attenuation values and iodine (water) concentrations for the lesions and aorta. Three recently introduced parameters were derived from the iodine concentration measurements and monochromatic images: (a) normalized iodine concentration (NIC), calculated as $NIC = IC_{lesion}/IC_{aorta}$, where IC_{lesion} and IC_{aorta} are the iodine concentrations in the lesions and in the aorta; iodine concentrations in the lesions were normalized to those of the aorta in order to minimize variations in patients; (b) the slope of the spectrum curve (λ_{HU}), calculated as $\lambda_{HU} = (CT_{40\ keV}\text{-}CT_{140\ keV})/100$, where $CT_{40\ keV}$ and $CT_{140\ keV}$ are the CT attenuation values of the tumors on 40 keV and 140 keV monochromatic images, respectively; and (c) CT value difference, which is the difference between the AP and VP of CT attenuation values of the tumors on 70 keV.

Qualitative analysis

Two radiologists (XYJ and ZJL with 7 and 25 years of experience, respectively) who were blinded to the diagnosis of the lesion, patient information, and results of the correlative imaging examinations qualitatively reviewed the CT images in consensus at a workstation. The readers recorded the following lesion features:

location (unilateral or bilateral), margin of mass (smooth, lobulated), necrosis, calcification, presence of swollen mediastinal lymph nodes, relationship with adjacent vessels, enhancement pattern, and degree on 70 keV monochromatic images. Necrosis was defined as either the presence or absence of areas within the tumor that did not demonstrate contrast enhancement during both AP and VP. The relationship with adjacent vessels was described as compression or wrap. The enhancement degree was described as mild or severe when the CT value increased by less than 20 HU or more than 20 HU, respectively. The changes in enhancement pattern between the phases were characterized as gradualness or washout. Gradualness was defined as a change from low attenuation during the AP to high attenuation during the VP, and washout was defined as a change from high attenuation during the AP to low attenuation during the VP.

Finally, in consensus, the readers characterized each lesion as a thymoma or mediastinal lymphoma on the basis of the imaging findings. Differences among the observers were resolved by means of consensus conference. The sensitivity (correct diagnosis of thymomas) and specificity (correct diagnosis of mediastinal lymphomas) of the individual phase were evaluated.

Statistical analysis

The data were analyzed using SPSS v. 22.0 (Chicago, IL). Quantitative values were recorded as the mean ± standard deviation. The two-sample *t*-test was performed to compare the quantitative parameters of NICs, λ_{HU}, and CT value difference between thymoma and mediastinal lymphoma, with $p < 0.05$ indicating statistical significance. Receiver operating characteristic (ROC) curves were generated for the values with statistically significant differences to evaluate their diagnostic efficiency and calculate the cut-off value, sensitivity, and specificity in the maximal Youden's index. The null hypothesis was that the area under the curve (AUC) was 0.5, and the alternative hypothesis was that AUC >0.5.

RESULTS

Quantitative image analysis

Two example set of images derived from a single spectral CT acquisition (section thickness, 1.25 mm) in a patient with thymoma is shown in Figure 1 and a patient with mediastinal lymphoma in Figure 2. Values for the defined quantitative parameters measured in the patients with thymoma and in those with mediastinal lymphoma are compared in Table 1. There were significant differences in NICs between the patients with thymoma and the patients with mediastinal lymphoma during the VP (mean NIC, 0.49 ± 0.15 mg ml^{-1} *vs* 0.28 ± 0.08 mg ml^{-1}; $p = 0.000$) (Figure 3a). The patients with thymoma had a significantly higher slope of the spectrum curve than did the patients with mediastinal lymphoma during the AP (mean λ_{HU}, 1.26 ± 0.74 *vs* 0.69 ± 0.17; $p = 0.001$) (Figure 3b). NIC during the AP, the λ_{HU} during the VP, and the CT value difference between the AP and VP of the two groups were not significantly different ($p > 0.05$).

The areas under the reader-specific ROC curves for all parameters (Figure 4) can be used to differentiate between thymoma and mediastinal lymphoma, especially the curves for the NICs during the VP (0.875).

Figure 1. Transverse (a) polychromatic CT images and (b) monochromatic CT image obtained at 70-keV energy level and (c) water-based and (d) iodine-based material decomposition images obtained from spectral CT acquisition (section thickness, 1.25 mm) in 49-year-old female with thymoma.

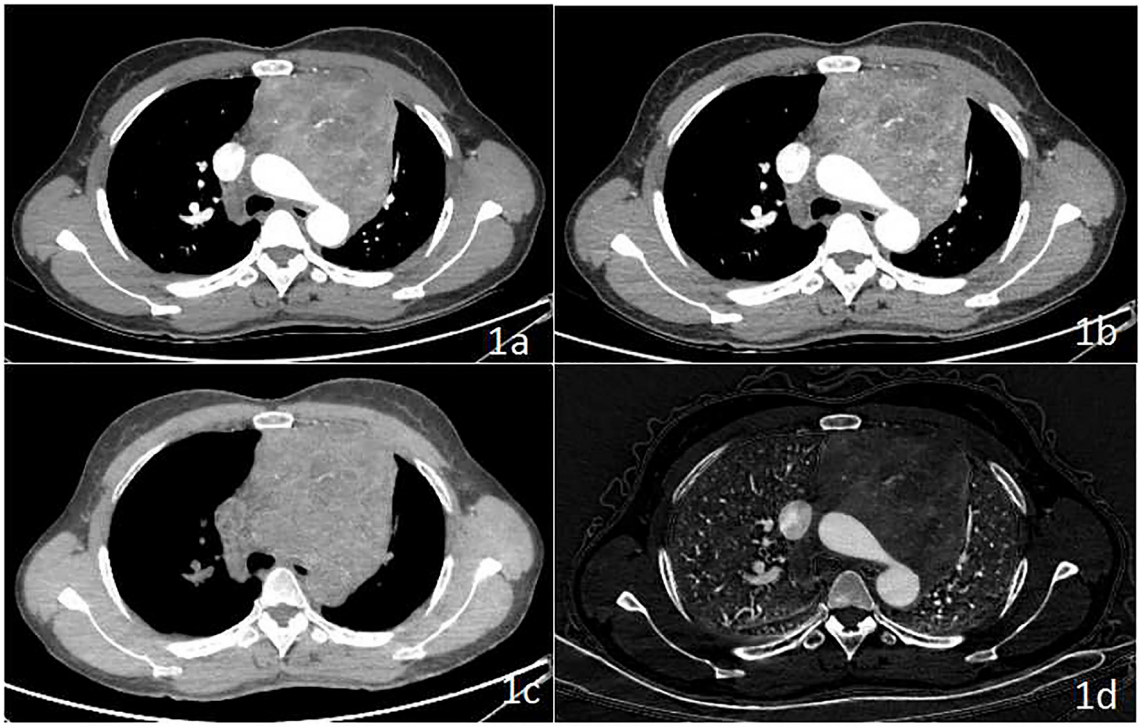

Figure 2. Transverse (a) polychromatic CT images and (b) monochromatic CT image obtained at 70-keV energy level and (c) water-based and (d) iodine-based material decomposition images obtained from spectral CT acquisition (section thickness, 1.25 mm) in 29-year-old male with mediastinal lymphoma.

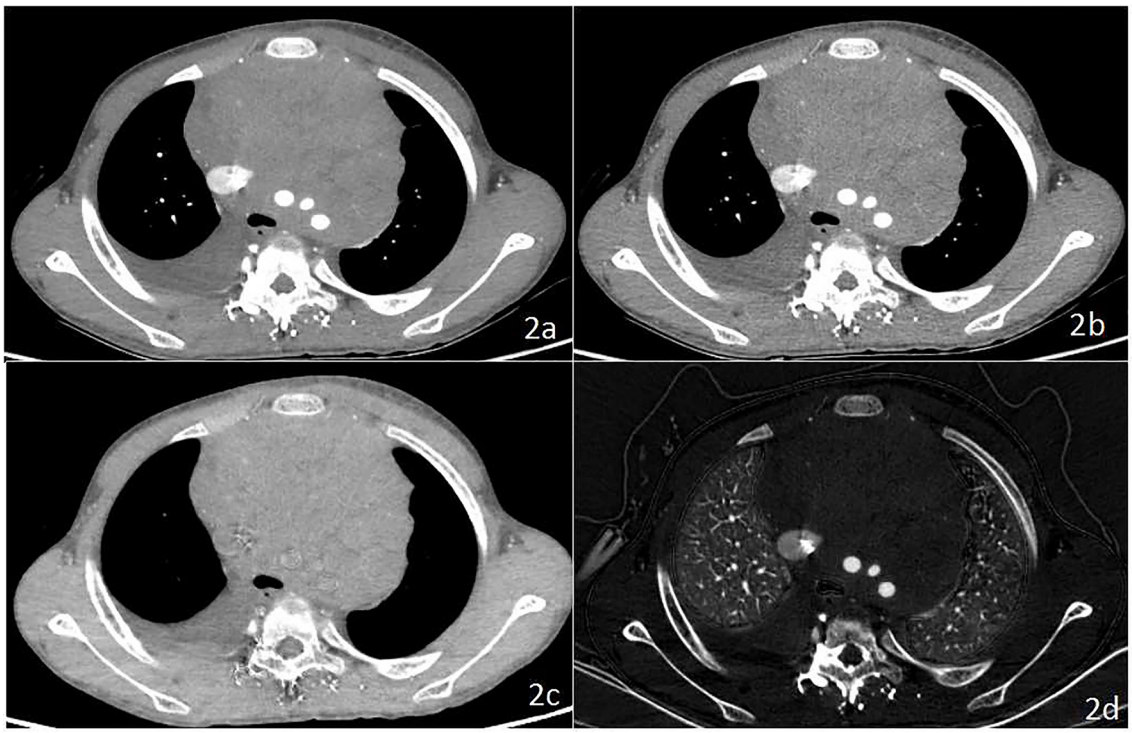

By using the ROC, we determined the parameter threshold values required to optimize both the sensitivity and specificity for differentiating between thymoma and mediastinal lymphoma (Table 2). For example, during the VP, a threshold NIC of 0.35 mg ml^{-1} would yield a sensitivity and specificity of 79.2% (19 of 24 thymomas) and 86.7% (13 of 15 mediastinal lymphomas), respectively, for differentiating between thymoma and mediastinal lymphoma. However, during the AP, a threshold λ_{HU} of 0.865 would decrease the sensitivity to 70.8% (17 of 24 thymomas) but increase the specificity to 93.3% (14 of 15 mediastinal lymphomas).

Table 1. Quantitative assessment of thymoma and mediastinal lymphoma at CT spectral imaging

Parameter	Thymoma	Mediastinal lymphoma	*p*-value
NIC–AP	0.14 ± 0.09	0.16 ± 0.12	0.661
λ_{HU}–AP	1.26 ± 0.74	0.69 ± 0.17	0.001
NIC–VP	0.49 ± 0.15	0.28 ± 0.08	<0.001
λ_{HU}–VP	1.37 ± 0.42	1.44 ± 1.22	0.803
CT value difference	1.52 ± 19.9	−8.11 ± 10.6	0.093

AP, arterial phase; NIC, normalized iodine concentrations; VP, venous phase.
With exception of *p* values, data are mean values ± standard deviations.

In terms of the selected combinations of optimal thresholds, the combination of NICs during the VP and λ_{HU} during the AP (0.35 mg ml^{-1} and 0.865, respectively) yielded optimal sensitivities and specificities of 79.2 and 93.3%, respectively, for differentiating between thymoma and mediastinal lymphoma.

Qualitative image analysis

The results of the qualitative analysis of monochromatic images are provided in Table 3. The location, margin, area of necrosis, presence of swollen mediastinal lymph nodes, relationship with adjacent vessels, and enhancement pattern differed between thymoma and mediastinal lymphoma ($p < 0.05$). The calcification and enhancement degree between the two were similar ($p > 0.05$). Using these qualitative criteria, we achieved a sensitivity and specificity of 68 and 73%, respectively.

DISCUSSION

Thymoma and lymphoma are the two most common types of tumors in the anterior mediastinum. The diagnosis of thymoma or mediastinal lymphoma can usually be based on their different clinical symptoms and imaging characteristics. However, clinical features of a number of cases are atypical, and diagnosis relies on medical imaging. There is considerable overlap between the imaging manifestation of anterior mediastinal lymphoma and thymoma, and it is difficult to differentiate the diagnosis; further, there are large differences between the treatments for thymoma and lymphoma. Therefore, the correct pre-operative differential diagnosis of thymoma and lymphoma is of great significance.

Figure 3. Box plots of (A) NIC during VP and (B) λ_{HU} during AP for thymomas and mediastinal lymphomas. AP, arterial phase; NIC, normalized iodine concentrations; VP, venous phase.

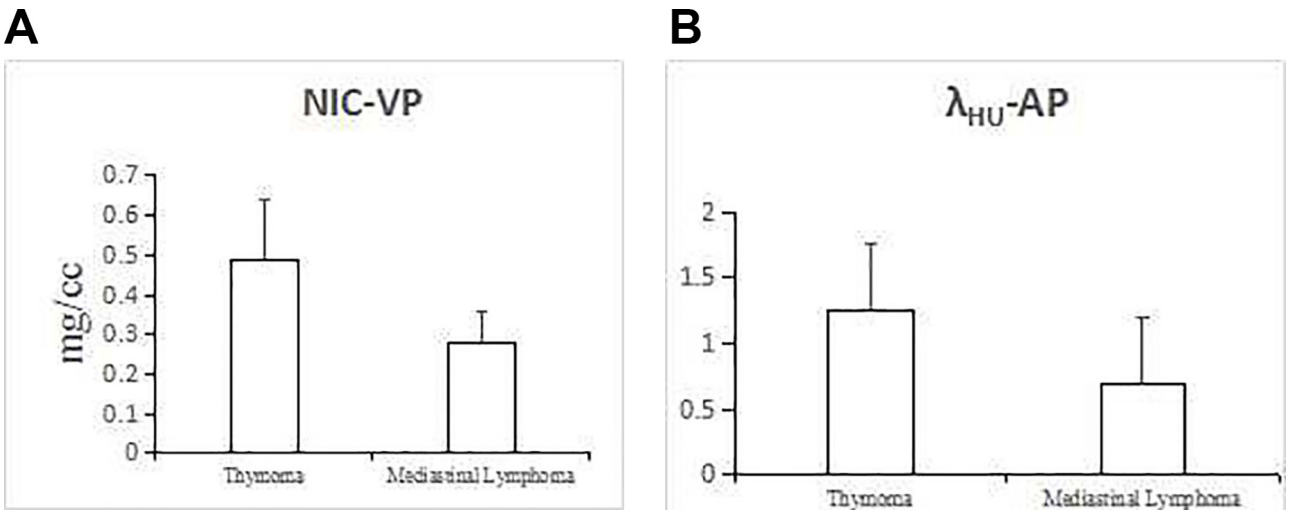

CT is the imaging modality of choice for evaluating thymoma and can help distinguish thymoma from other anterior mediastinal abnormalities.[1] In previous studies,[10,11] the role of CT in the diagnosis of thymoma and mediastinal lymphoma has been discussed, but most studies were focused mainly on qualitatively analyzing the imaging features of the lesions, and few have conducted quantitative analyses.

The averaging attenuation effect of polychromatic X-rays in conventional CT reduces the low-contrast spatial resolution between materials.[12] In addition, the use of a monochromatic X-ray beam in CT would eliminate the beam-hardening artifacts and average the attenuation effects.[13] CT spectral imaging yields monochromatic images that depict how an imaged object would look if the X-ray source produced only single-energy X-ray photons. This would facilitate increased contrast spatial resolution.

Figure 4. ROC curves for NIC during the VP and λ_{HU} during the AP in differentiating thymoma from mediastinal lymphoma. AP, arterial phase; NIC, normalized iodine concentrations; ROC, receiver operating characteristic; VP, venous phase.

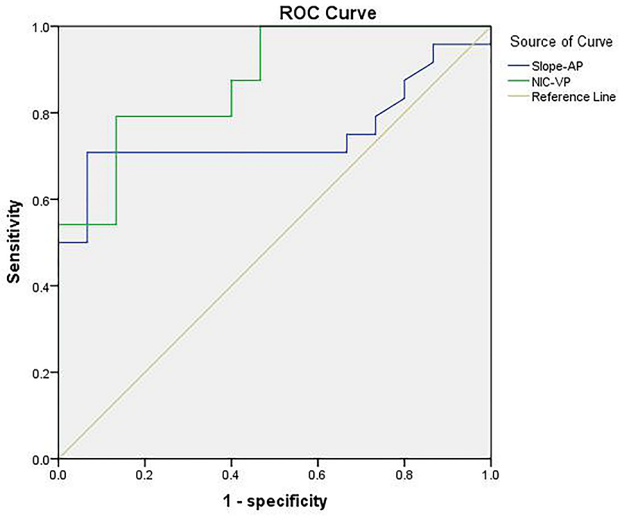

For medical diagnostic imaging, water and iodine are often selected as the basis pair for material-decomposition image presentation because their atomic numbers span the range of atomic numbers for the materials that are generally found in medical imaging. Additionally, water and iodine approximate the atomic numbers of soft tissue and iodinated contrast material to result in material-attenuation images that are intuitive to interpret. An *in vitro* experiment[12] demonstrated that the iodine concentration in lesions derived from the iodine-based material-decomposition images is quantitative and might thus be a useful parameter.

According to our study results, the iodine concentration was higher in enhancing thymomas than in enhancing mediastinal lymphomas during the VP. Additionally, the λ_{HU} values during the AP for thymomas were higher than were those for mediastinal lymphomas. However, we did not observe significant differences in iodine concentration during the AP. This finding indicates that in the venous phase, the blood supply (contrast agent concentration) of thymoma is higher than that of lymphoma. Histologically, thymomas are composed of neoplastic epithelial cells of thymus intermingled with non-neoplastic immature *T* lymphocytes (thymocytes),[14] which are separated by fibrous bands into lobules and contain prominent perivascular spaces.[15] Due to the existence of the above fiber septa, the speed of withdrawal of contrast agent decreases, and there is a higher iodine concentration during the VP. A lymphoma often infiltrates into vessel walls or between individual cells of mediastinal fat tissue and usually lacks a fibrous capsule or interlobular septa; hence, the contrast agent enters the tumor blood vessels during the arterial phase and exits rapidly during the venous phase.

Our study shows that the slope of the spectrum curve exhibited significant differences between thymoma and mediastinal lymphoma during the AP. The spectral curve reflects the material

Table 2. Thresholds, sensitivities, and specificities for distinguishing thymoma from mediastinal lymphoma

Parameter	AUC	Threshold	Sensitivity	Specificity
λ_{HU}-AP	0.750	0.865	70.8 (17)	93.3 (14)
NIC-VP	0.875	0.35	79.2 (19)	86.7 (13)

AP, arterial phase; AUC, area under the curve ; NIC, normalized iodine concentrations; VP, venous phase.
Sensitivity values are cited as percentages. Data in parentheses are numbers of thymoma (n = 24) used to calculate percentages. Specificity values are cited as percentages. Data in parentheses are numbers of mediastinal lymphoma (n = 15) used to calculate percentages.

CT value varying with the energy of the X-ray and the absorption characteristics to the different energies of X-rays. Various substances exhibit changes in chemical molecular structures, and different chemical molecules have modified energy attenuation curves.[16] Thus, we can distinguish the chemical composition of substances by comparing the slopes of the spectrum curves.[17] This may have occurred because thymomas can be cystic in nature, which has been identified through histopathology and correlates with gross pathology,[18] but the predominantly solid appearance of lymphomatous lymph nodes suggests that the tumor cells are closely arranged. Such different histological structures between thymoma and lymphoma lead to different absorption characteristics.

In our study, the ROC curves analysis revealed that the combination of NICs during the VP and λ_{HU} during the AP (0.35 mg ml^{-1} and 0.865, respectively) yielded optimal sensitivities and specificities of 79.2 and 93.3%, respectively, for differentiating between thymoma from mediastinal lymphoma. Compared with qualitative imaging analysis, quantitative analysis with spectral CT improved both the sensitivity (from 68 to 79.2%) and specificity (from 73 to 93.3%). However, the threshold values evaluated in our study were based on specific populations, and the accuracy of these values requires further confirmation by using larger sample sizes in future studies.

Our study did have limitations. First, the study sample size was small, and the results were preliminary and thus require verification in additional studies performed with more lesions. Second, the study did not compare the different pathological grading of thymoma with different subtype lymphomas, and further studies will be conducted with expanded samples.

In conclusion, CT spectral imaging enables the material decomposition and analysis of a number of additional quantitative CT imaging parameters, namely the NIC and slope of the spectrum curve, which may help increase the accuracy of differentiating thymoma from mediastinal lymphoma and thus help guide clinical treatment.

Table 3. Qualitative CT assessment of lesions

CT signs		Thymoma (24)		Mediastinal lymphoma (15)		X^2-value	p-value
		n	%	N	%		
Location	Unilateral	20	83.3	3	20	15.303	<0.001
	Bilateral	4	16.7	12	80		
Margin	Smooth	16	66.7	4	26.7	5.912	0.015
	Lobulated	8	33.3	11	73.3		
Calcification	Yes	2	8.3	0	0		0.514[a]
	No	22	91.7	15	100		
Necrosis	Yes	18	75	6	40	4.778	0.029
	No	6	25	9	60		
Swollen mediastinal lymph nodes	Yes	3	12.5	11	73.3	14.845	<0.001
	No	21	87.5	4	26.7		
Relationship with adjacent vessels	Compression	19	79.2	4	26.7	10.516	0.001
	Wrap	5	20.8	11	73.3		
Enhancement degree	Mild	11	45.8	9	60	0.742	0.389
	Server	13	54.2	6	40		
Enhancement pattern	Gradualness	4	16.7	10	66.7	10.209	0.002
	Washout	20	83.3	5	33.3		

Data are numbers of lesions and percentages. $p < 0.05$ indicates a statistically significant difference between thymoma and mediastinal lymphoma.
Expected count <5, use Fisher's exact test.

ACKNOWLEDGMENT

This work was supported by Talent Innovation and Entrepreneurship Project of Lanzhou (No.2016-RC-58), and Natural Science Foundation Project of Gansu Province (No.17JR5RA253).

ETHICS APPROVAL

All procedures performed in studies involving human participants were in accordance with the ethical standards of the institutional research committee and with the 1964 Helsinki declaration and its later amendments or comparable ethical standards.

CONSENT

Informed consent was obtained from all individual participants included in the study.

REFERENCES

1. Benveniste MF, Rosado-de-Christenson ML, Sabloff BS, Moran CA, Swisher SG, Marom EM. Role of imaging in the diagnosis, staging, and treatment of thymoma. *Radiographics* 2011; **31**: 1847–61. doi: https://doi.org/10.1148/rg.317115505
2. Girard N, Mornex F, Van Houtte P, Cordier JF, van Schil P, Houtte PV. Thymoma: a focus on current therapeutic management. *J Thorac Oncol* 2009; **4**: 119–26. doi: https://doi.org/10.1097/JTO.0b013e31818e105c
3. Priola AM, Galetto G, Priola SM. Diagnostic and functional imaging of thymic and mediastinal involvement in lymphoproliferative disorders. *Clin Imaging* 2014; **38**: 771–84. doi: https://doi.org/10.1016/j.clinimag.2014.05.012
4. Zieliński M, Czajkowski W, Gwozdz P, Nabiałek T, Szlubowski A, Pankowski J. Resection of thymomas with use of the new minimally-invasive technique of extended thymectomy performed through the subxiphoid-right video-thoracoscopic approach with double elevation of the sternum. *Eur J Cardiothorac Surg* 2013; **44**: e113–e119. doi: https://doi.org/10.1093/ejcts/ezt224
5. Lisenko K, Dingeldein G, Cremer M, Kriegsmann M, Ho AD, Rieger M, et al. Addition of rituximab to CHOP-like chemotherapy in first line treatment of primary mediastinal B-cell lymphoma. *BMC Cancer* 2017; **17**: 359. doi: https://doi.org/10.1186/s12885-017-3332-3
6. Wu LM, Li YL, Yin YH, Hou GQ, Zhu R, Hua XL, et al. Usefulness of dual-energy computed tomography imaging in the differential diagnosis of sellar meningiomas and pituitary adenomas: preliminary report. *PLoS One* 2014; **9**: e90658. doi: https://doi.org/10.1371/journal.pone.0090658
7. Fischer MA, Gnannt R, Raptis D, Reiner CS, Clavien PA, Schmidt B, et al. Quantification of liver fat in the presence of iron and iodine: an ex-vivo dual-energy CT study. *Invest Radiol* 2011; **46**: 351–8. doi: https://doi.org/10.1097/RLI.0b013e31820e1486
8. Yu Y, Lin X, Chen K, Chai W, Hu S, Tang R, et al. Hepatocellular carcinoma and focal nodular hyperplasia of the liver: differentiation with CT spectral imaging. *Eur Radiol* 2013; **23**: 1660–8. doi: https://doi.org/10.1007/s00330-012-2747-0
9. Qian LJ, Zhu J, Zhuang ZG, Xia Q, Cheng YF, Li JY, et al. Differentiation of neoplastic from bland macroscopic portal vein thrombi using dual-energy spectral CT imaging: a pilot study. *Eur Radiol* 2012; **22**: 2178–85. doi: https://doi.org/10.1007/s00330-012-2477-3
10. Guan W, Yuan Y, Liu X. Different signs CT diagnosis and differential diagnosis of mediastinal thymoma and common malignancy. *Journal of Modern Oncology* 2015.
11. Matsumoto T, Shimabukuro M, Okita I, Hirose T, Yamakawa K, Nakamura H, et al. CT findings of malignant lymphoma of the anterior mediastinum-differentiation from invasive thymoma. *Nihon Igaku Hōshasen Gakkai Zasshi Nippon Acta Radiologica* 1989; **49**: 414.
12. Lv P, Lin XZ, Li J, Li W, Chen K. Differentiation of small hepatic hemangioma from small hepatocellular carcinoma: recently introduced spectral CT method. *Radiology* 2011; **259**: 720–9. doi: https://doi.org/10.1148/radiol.11101425
13. Lin XZ, Wu ZY, Tao R, Guo Y, Li JY, Zhang J, et al. Dual energy spectral CT imaging of insulinoma-Value in preoperative diagnosis compared with conventional multi-detector CT. *Eur J Radiol* 2012; **81**: 2487–94. doi: https://doi.org/10.1016/j.ejrad.2011.10.028
14. Szolkowska M, Langfort R, Winiarski S, Zaremba J, Prochorec-Sobieszek M, Rymkiewicz G, et al. Two neoplasms rich in small lymphocytes, B1B2 thymoma and small lymphocytic lymphoma, intermingled in one tumor mass. A case report. *Pol J Pathol* 2017; **68**: 75–81. doi: https://doi.org/10.5114/pjp.2017.67620
15. Moran CA, Suster S, Fishback NF, Koss MN. Primary intrapulmonary thymoma. A clinicopathologic and immunohistochemical study of eight cases. *Am J Surg Pathol* 1995; **19**: 304–12.
16. Karçaaltıncaba M, Aktaş A. Dual-energy CT revisited with multidetector CT: review of principles and clinical applications. *Diagn Interv Radiol* 2011; **17**: 181–94. doi: https://doi.org/10.4261/1305-3825.DIR.3860-10.0
17. Graser A, Johnson TR, Chandarana H, Macari M. Dual energy CT: preliminary observations and potential clinical applications in the abdomen. *Eur Radiol* 2009; **19**: 13–23. doi: https://doi.org/10.1007/s00330-008-1122-7
18. Patterson MM, Marolf AJ. Sonographic characteristics of thymoma compared with mediastinal lymphoma. *J Am Anim Hosp Assoc* 2014; **50**: 409–13. doi: https://doi.org/10.5326/JAAHA-MS-6132